Research on Hydraulic Power System Operation Status Diagnosis Technology Based on Hybrid CNN Model

Rundong Shen, Kechang Zhang* and Jinyan Shi

Hunan Railway Professional Technology College, ZhuZhou 412001, China
E-mail: zhangkechang2008@163.com
**Corresponding Author*

Received 20 September 2022; Accepted 18 October 2022;
Publication 26 November 2022

Abstract

Aiming at the problems that the features extracted from the traditional system operation state are not adaptive and the specific system operation state is difficult to match, a gearbox system operation state diagnosis method based on continuous wavelet transform (CWT) and two-dimensional convolutional neural network (CNN) is proposed. The method uses the continuous wavelet transform to construct the time-frequency map of the hydrodynamic system operating state signal, and uses it as the input to construct a convolutional neural network model, and forms a deep distributed system operating state feature expression through a multilayer convolutional pool. The structural parameters of each layer of the network are adjusted by the back propagation algorithm to establish an accurate mapping from the signal characteristics to the system operating state. In the experiments under different working conditions and different system operation states, the accuracy of system

European Journal of Computational Mechanics, Vol. 31_3, 387–408.
doi: 10.13052/ejcm2642-2085.3133

operation state recognition reaches 99.2%, which verifies the effectiveness of the method. Using this method of adaptively learning rich information in the signal can provide a basis for intelligent system operation state diagnosis.

Keywords: Gearbox, CWT, time-frequency diagram, system operating condition diagnosis, CNN.

1 Introduction

Hydraulic equipment is playing an increasingly dominant role in mechanical engineering power and automation. However, the higher the power and automation, the more complex the structure of the equipment, the greater the possibility of system operating conditions, and the greater the hazards and losses caused by system operating conditions [1]. Taking the hydraulic power system in mechanical engineering as the object, on the basis of theoretical analysis and a large number of experimental research, four standard operating modes of hydraulic power system based on the power spectrum characteristics of current signal are given. A pattern recognition method based on grey correlation degree calculation is proposed, which can well identify the normal hydraulic power system and the occurrence of motor fault, machine fault and oil pump fault. In addition, the grey correlation degree algorithm is simple and the amount of calculation is small, which can realize online monitoring. Therefore, it is especially important to monitor the operating status of the hydraulic system in a timely and effective manner and to accurately determine the causes of the operating status of the system. The use of units hope that the equipment of the mechanical and electrical devices in the process of operation can operate normally, once the overload, impact, jamming and other unexpected system operating conditions can be dealt with in a timely manner, otherwise it will lead to equipment damage, causing significant economic losses to the use of units. Therefore, the manufacturers are trying to improve the reliability of the equipment at the same time, hope to find an economical and practical condition monitoring method, to prevent problems before they occur, to achieve scientific management [2].

Some scholars have already studied the end-to-end system operation status diagnosis method that unifies feature extraction and shallow machine learning classification under one framework and extracts features directly from the original signals. In [3], a stacked denoising automatic coding method was proposed to diagnose the operating status of rolling bearing

systems. In [4], a rough set attribute reduction based on mutual information is introduced to optimize the decision tree classification algorithm, and it is used for aero-engine oil-hydraulic system operating condition diagnosis. [5] used deep confidence networks (DBN) to fuse multi-sensor information and applied it to aero-engine structural health status identification. [6] used the empirical modal decomposition (EMD) method to process the input to obtain multichannel one-dimensional signals. These methods provide useful references for automatic learning of system operating state features, but they all learn from a single time or frequency domain, and the learned features cannot yet portray the two-dimensional characteristics of the system operating state.

Learning algorithms that use the extracted features to train classifiers for state recognition include K-nearest neighbor classifier (KNN) [7], artificial neural network (ANN) [8], support vector machine (SVM) [9], wavelet clustering (WCG) [10], and so on. In recent years, convolutional neural networks (CNNs) in deep learning algorithms have become a hot research topic because of their ability to automatically extract and integrate signal features, and their feature representation capability improves with the increase of network layers. In [11], a deep adversarial convolutional CNN was proposed for variable working conditions of gearboxes to improve the generalization performance of the network. [12] designed a deep coupled dense convolutional network (deep coupled dense CNN) for the gradient disappearance problem to better characterize the system operation state of the gearbox input signal. [13] proposed a convolutional gated recurrent neural network-based diagnostic model for the operating state of a bearing system, which solves the problem of degraded diagnostic performance under small sample data. The method of input processing signal to CNN has higher accuracy compared with the CNN of input raw signal, a fault diagnosis method based on the combination of DBN and 1D CNN proposed by [14], and a system running state diagnosis method based on the combination of EMD, SVM and CNN studied by [15].

In this paper, we propose a model to diagnose the operating condition of gearbox system by combining CWT and 2D-CNN. Based on the rich information in the CWT time-frequency map, the CNN adaptively learns the time-frequency features to avoid the manual extraction of system operation status features, and automatically optimizes the network according to the classification and diagnosis errors, which can provide the basis for the intelligent implementation of system operation status diagnosis by organically integrating feature extraction and feature classification [16].

2 Identification Mechanism Analysis

2.1 Dynamics Model of Hydraulic Power System

The electro-mechanical-hydraulic coupling mode of the motor-driven oil pump rotor system is shown in Figure 1. The most fundamental guiding ideology of modeling with system dynamics method is the system view and methodology of system dynamics. System dynamics believes that the system has integrity, correlation, hierarchy and similarity. The internal feedback structure and mechanism of the system determine the behavior characteristics of the system. Any complex large-scale system can be connected by the most basic information feedback loops of multiple systems in some way. The system goal of system dynamics model is to solve system problems from the perspective of change and development according to the actual application. One of the most important characteristics of system dynamics modeling and simulation is to realize the dual simulation of structure and function. Therefore, the correct implementation of the principle of system decomposition and system synthesis must run through the whole process of system modeling, simulation and testing. Like other models, the system dynamics model is only the simplification and representation of some essential characteristics of the actual system, rather than the original local translation or replication. Therefore, in the process of constructing system dynamics model, we must pay attention to grasp the overall situation, grasp the main contradictions, reasonably define system variables and determine system boundaries. There are a whole set of qualitative and quantitative methods to test the consistency and effectiveness of system dynamics models, such as sensitivity analysis of structures and parameters, simulation tests under extreme conditions and statistical method tests, etc., but the final standard to evaluate the quality of a model is objective practice, and the practical test is long-term, and it can not

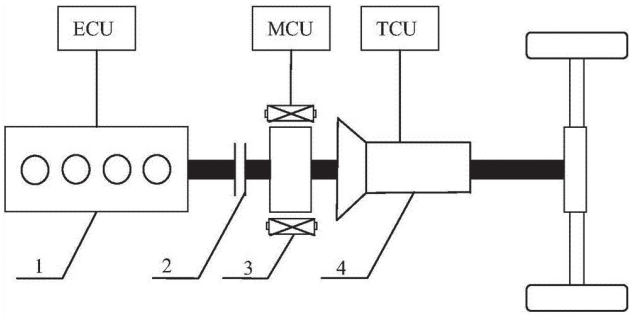

Figure 1 Dynamics model of the motor-driven oil pump rotor system.

be completed once or twice. Therefore, even a carefully constructed model must be constantly modified and improved in future applications to adapt to the new changes and new goals of the actual system.

The motor shaft and the oil pump rotor are coupled by a flexible coupling, and the motor and the oil pump base are considered rigid. During the operation of the system, the rotor system will vibrate relative to the ground (x, y) direction due to eccentricity or misalignment, in addition to torsional vibration (δ direction) relative to the motor shaft during unstable processes such as starting, braking, and oil shock. When torsional vibration occurs, the and of the motor shaft and the oil pump shaft will change continuously. Since the rotational speed of the motor shaft is constantly changing during the unstable process, it is convenient to use the synchronous constant speed rotational coordinate system (MT) to describe the operating state of the motor system [17].

The modeling process of system dynamics is a process of understanding and solving problems. According to the law of people's understanding of objective things, it is a process of wavy progress and spiral rise. Therefore, it must be a process from coarse to fine, from outside to inside, repeated cycles and deepening. System dynamics sums up the whole modeling process into five steps: system analysis, structure analysis, model establishment, model test and model use. These five steps have a certain order, but according to the specific situation in the modeling process, they are all cross and repeated. The main task of the first step of system analysis is to clarify the system problems, widely collect the relevant data, information and information to solve the system problems, and then roughly delineate the boundary of the system. The second step of structural analysis focuses on the structural decomposition of the system, the determination of system variables and the information feedback mechanism. The third step is the quantitative process of system structure (establishing model equations for quantification). The fourth step of model test is to simulate and debug the model with the help of computer, and constantly modify and improve the model through the evaluation of various performance indicators of the model. The fifth step of model use is to conduct quantitative analysis and Research on system problems and do various policy experiments on the established model.

The equation of motion of the oil pump rotor system is

$$\begin{aligned} m\ddot{x} + c_x x + k_x x &= me(\sin\theta - \theta_{\cos})\theta m\ddot{y} + c_y y' + k_y y - mg \\ &= \theta_m e - \theta_{os}\theta + \cdot\theta_{\sin}\theta(J_{\mathrm{p}} + \mathrm{me}^2)\cdot\theta \end{aligned} \tag{1}$$

According to the hydraulic transmission theory, the torque equation of the oil pump is

$$M_{\mathrm{p}} = \frac{p_{\mathrm{p}} q}{2\pi_{\mathrm{p}}^{\eta}} \tag{2}$$

According to the motor theory, the voltage equation of a three-phase asynchronous motor in MT coordinate system is expressed as follows:

$$\begin{bmatrix} u_M \\ u_T \\ 0 \\ 0 \end{bmatrix} = \begin{bmatrix} r_{\mathrm{s}} + \Delta_{\mathrm{s}} & \omega L_{\mathrm{s}} & \Delta_{\mathrm{m}} & \omega L_{\mathrm{m}} \\ -\omega L_{\mathrm{s}} & r_{\mathrm{s}} + \Delta L_{\mathrm{s}} & -\omega L_{\mathrm{m}} & \Delta L_{\mathrm{m}} \\ \Delta_{\mathrm{m}} & (\omega - \omega) L_{\mathrm{m}} & r_{\mathrm{r}} + \Delta_{\mathrm{r}} & (\omega_{\mathrm{s}} - \omega_{\mathrm{r}}) L_{\mathrm{r}} \\ (\omega - \omega) L_{\mathrm{m}} & \Delta_{\mathrm{m}} & -(\omega - \omega) L_{\mathrm{r}} & r_{\mathrm{r}} + \Delta_{\mathrm{r}} \end{bmatrix} \times \begin{bmatrix} \dot{i}_M \\ \dot{I}_{\mathrm{T}} \\ \dot{i}_{\mathrm{m}} \\ \dot{I}_{\mathrm{t}} \end{bmatrix} \tag{3}$$

The equation of motion of the rotor of the motor is

$$\frac{J_e}{p} \frac{d\omega}{dt} = \mathrm{e} - \mathrm{k}_{\delta} \delta \tag{4}$$

The following equilibrium relationship exists between the angular velocity of the motor spindle and the mechanical rotor

$$\frac{\mathrm{d}}{\mathrm{d}t} \delta = \overset{\omega}{p} - \theta \tag{5}$$

Substituting the previous equation into Equation (3) yields

$$\begin{aligned} &(J_{\mathrm{p}} + \mathrm{m}e^2) \cdot \theta \underline{\overset{2}{3}} p L_{\mathrm{m}} (i_{\mathrm{T}} i_m - i_M i_{\mathrm{t}}) \overset{J_{\mathrm{e}}}{p} \frac{\mathrm{d}\omega_{\mathrm{t}}}{\mathrm{d}t} - \frac{p_p q}{2\pi_p^{\eta}} \\ &\quad + \mathrm{mexsin}\theta - me(\ddot{y} + g) \cos\theta \end{aligned} \tag{6}$$

2.2 Principle of Recognition Based on Current Signal

The hydraulic power system is generally driven by a three-phase asynchronous motor, and its current changes proportionally with the pump load during operation, so the electric control cabinet is generally equipped with a motor current monitoring device – current transformer, through which the effective value of the current change during the motor operation can

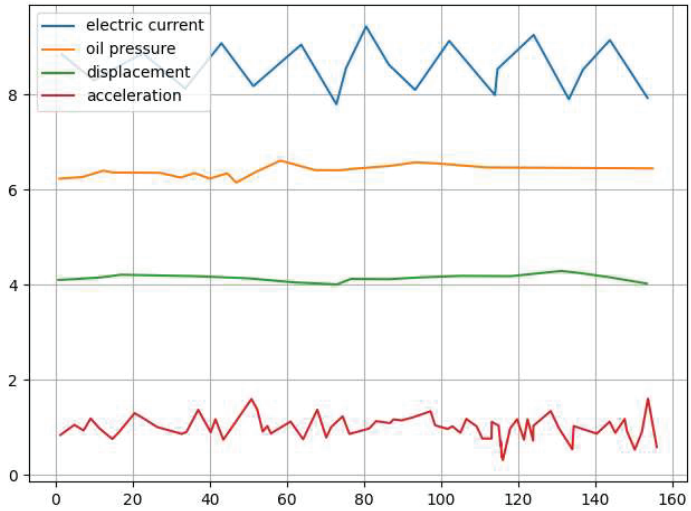

Figure 2 Overload working condition current, oil pressure, vibration signal change process.

be observed at any time. From the analysis of Equations (1) to (6), it is known that due to the coupling of rotor system, the current carries a lot of useful information reflecting the operation status of the equipment, if a suitable signal processing method is adopted, it will bring great convenience to the status monitoring and even system operation status identification. In the current transformer output and a resistor R on the current sensor, the voltage U is the output voltage of the current sensor, the analog voltage U by A/D conversion can be sent to the digital signal processing system for information processing [18].

Figure 2 shows the current, oil pressure, vibration displacement and acceleration signals measured simultaneously on the test system as a function of time. As seen in Figure 2.

(1) Overload overflow process, the current always exceeds the rated value, and the maximum peak than the maximum peak oil pressure lags 20∼30 ms, vibration parameters also increased, which indicates that the oil pump rotor system issued by the machine, electricity, liquid information has a strong coupling characteristics;
(2) When operating under rated load, the current, oil pressure and vibration signals change smoothly and have weak coupling characteristics.

In summary, due to the coupling effect of the electromechanical and hydraulic parameters of the rotor system, the current signal contains

information reflecting the operating status of the motor, hydraulic pump and mechanical device.

3 CWT-CNN System Operation Status Recognition Algorithm

The flow of system operation status diagnosis by CWT-CNN algorithm is shown in Figure 3. Firstly, the time-frequency map is obtained by continuous

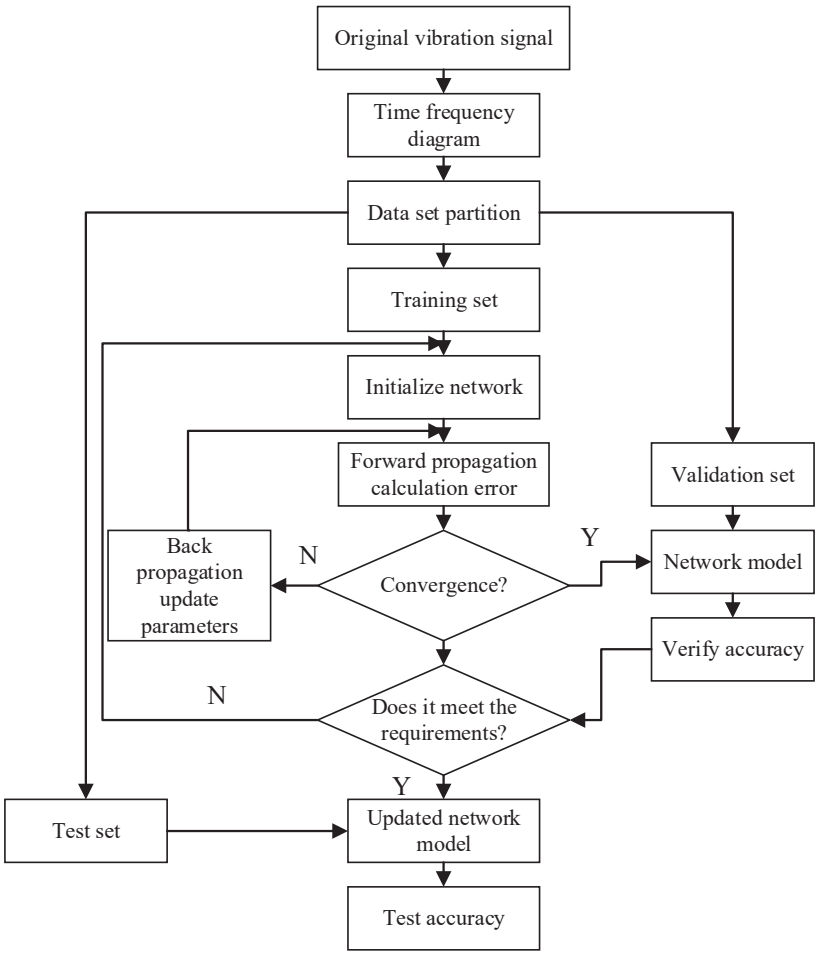

Figure 3 Flow of CWT-CNN system operation status diagnosis.

wavelet transform of the original vibration signal; then the forward and backward propagation algorithms of the convolutional network are used to learn the rich information in the time-frequency signal and obtain the time-frequency features related to the essence of the system operation state signal; finally, the classification layer of the network establishes the mapping relationship between the extracted features and the corresponding system operation state type. The image is the input layer, followed by CNN's unique convolution layer. The built-in activation function Q of the convolution layer uses relu, followed by CNN's unique pooled Q layer. The combination of 4 convolution layers + pooled layers can appear many times in the hidden layer. It can also be flexibly combined. Convolution + convolution + pooling, convolution + convolution, etc. 5 is the fully connected layer Q (fully connected layer) after several convolution layers + pooling layers, which is actually the DNN structure, but the output layer uses the softmax activation function to classify image recognition. Generally, FC is the full connected layer of CNN. The full connection layer generally includes the output layer that finally activates the function with softmax Q.

3.1 Continuous Wavelet Transform

The short-time Fourier transform (STFT) is one of the first proposed time-frequency analysis methods for nonlinear signals. The process is to first split the complete signal into a finite number of segments that can be considered as smooth signals through a window that keeps sliding with time, and then use the Fourier transform to analyze each segment of the signal, and finally stitch together the frequency features of all the time segments Then the Fourier transform is used to analyze each segment, and finally the frequency features of all time segments are stitched together to obtain a feature matrix that can describe the information of system operation in the signal. However, the shape of the window function in STFT is fixed, that is, when the window width is large, the frequency resolution is high but the time resolution is low; when the window width is small, the time resolution is high but the frequency resolution is low [19]. The time-frequency features generated using this method are difficult to perform effective system operation status diagnosis. For this reason, the CWT adjustable time-frequency window is used. For an arbitrary signal x(t), its continuous wavelet transform is

$$T_{\mathrm{cw},x}(u,v) = \int_{-\infty}^{+\infty} x(t)\varphi_{u,v}(t)\mathrm{d}t$$

$$= \frac{1}{\sqrt{v}} \int_{-\infty}^{+\infty} x(t)\varphi\left(\frac{t-u}{v}\right) \mathrm{d}t \tag{7}$$

$$\varphi_{u,v}(t) = \frac{1}{\sqrt{v}}\varphi\left(\frac{t-u}{v}\right), \quad v > 0,\ u \in R \tag{8}$$

The wavelet transform can automatically adjust the factors u and v by the characteristics of the signal, which makes the wavelet transform adaptive and multi-resolution for different time interval vibration signals of gearboxes.

3.2 Convolutional Neural Networks

The main structure of CNN includes input layer, convolutional layer, pooling layer, fully connected layer and output layer, as shown in Figure 4. The pooling layer connects one or more convolutional layers to form a convolutional pooling module, and multiple similar convolutional pooling modules are accumulated to obtain a deep network structure, which is connected into the fully connected layer to achieve label classification in the output layer. CNN extracts features from the input in layers, and the lower layers can learn generalized features such as contours in images, while the higher layers can integrate the low-level features into abstract high-level feature information [20].

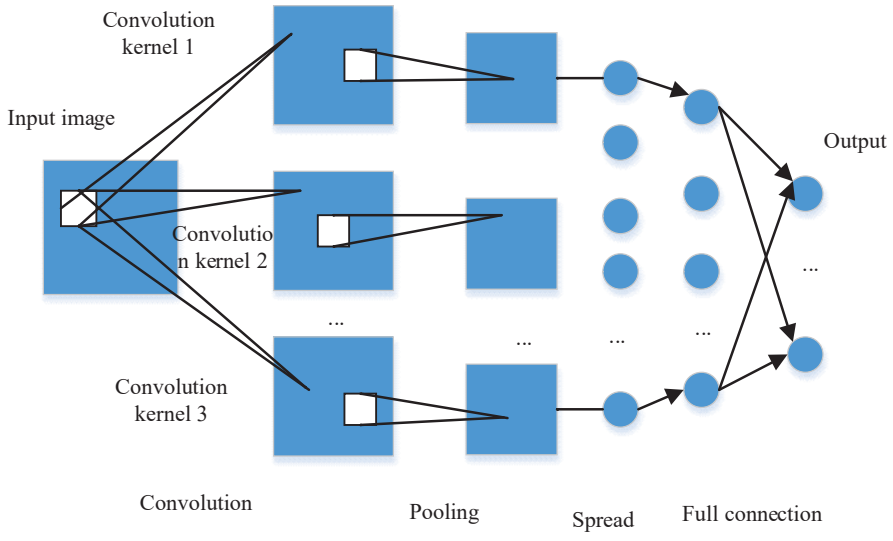

Figure 4 Convolutional neural network structure.

The learning training of the network is divided into two processes: forward propagation and backward propagation. The forward propagation process is to input the sample data into the network, and the output of the network is obtained through the layer-by-layer computational propagation of the network. The backward propagation process aims to reduce the loss function, adjust the structural parameters in the network and update the network parameters.

The pooling layer operation is

$$O^{l+1} = F_{\text{pool}}(A^l) \tag{9}$$

Where O^{l+1} is the output of the $1 + 1$ layer pooling; A^l is the output of the lth convolutional layer activation; $F_{\text{pool}}(\cdot)$ is the pooling function.

The features extracted from the multilayer convolutional pooling block are classified in the fully connected layer, and the probabilistic output corresponding to the input is obtained in the output layer using the Softmax activation function, whose expression

$$q = \text{Softmax}(\mathbf{Z}^l) = \frac{\text{e}^{Z'}}{\sum_{k=1}^{c} \text{e}^{Z'_{i-1},\ldots,m,k}} \tag{10}$$

Where q is the output after activation; m is the number of input samples; c is the number of output categories, and Softmax$(\cdot)$ is the activation function.

3.3 CWT-CNN Model Construction

The main structure of CNN includes input layer, convolutional layer, pooling layer (sampling layer), fully connected layer and output layer. In the proposed CWT-CNN model, the input layer is the time-frequency signal obtained by continuous wavelet transform of the vibration signal, and the features are extracted by each convolutional layer and reduced by each pooling layer, and then the features are recombined by the fully connected layer, and finally the system operation state recognition results are output by the classifier function. The model adjusts the number of convolutional layers according to the recognition accuracy on the training and test sets. When the accuracy on the training set is low, the underfitting of the model is reduced by increasing the number of layers or increasing the number of channels per layer; when the accuracy on the training set is high but the accuracy on the test set is low, the overfitting of the model is reduced by decreasing the number of layers or regularization.

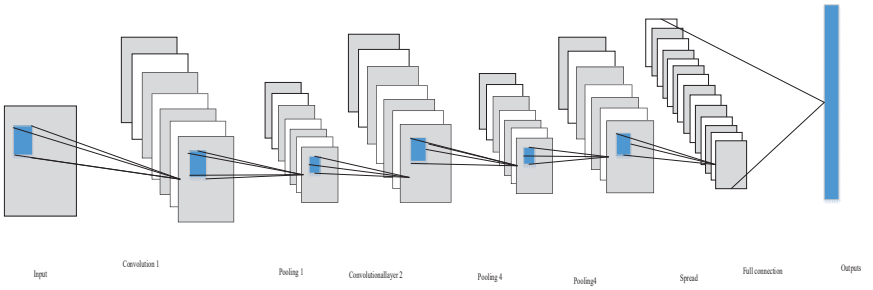

Figure 5 CNN structure of CWT-CNN model.

The CNN model depends on the selection of hyperparameters (learning rate, Dropout rate, number of channels, number of layers, minimum batch size) and training methods (pooling method, activation function, backpropagation optimization algorithm). The initial learning rate is set to 0.001; the pooling layer adopts the maximum pooling method to avoid the offset of the estimated mean value caused by the small change of the convolution kernel; the activation function is selected as ReLU function; the dropout probability of Dropout regularization is adjusted to 0.2; the Adam algorithm is used for model training optimization, and the parameters are set as $\beta_1 = 0.9$, $\beta_2 = 0.999$, $\varepsilon = 10^{-8}$; the minibatch size is set as the parameters of each layer structure are shown in Table 1, where the increasing number of channels indicates the multi-dimensional extraction of high-dimensional features; the "zero complement" means filling elements on both sides of the height and width of the input, thus controlling the shape of the output.

3.4 Objective Function

The LCD method assumes that any complex signal can be decomposed into the sum of several endogenous scale components with physically meaningful instantaneous frequencies, and the decomposition process is as follows:

$$\mathrm{r(t)} = \mathrm{x(t)},\ \mathrm{i} = 0 \tag{11}$$

(2) Determine the extremum $(\tau_k, X_k)(k = 1, 2, \ldots, M)$ of signal $r_i(t)$ and calculate

$$\begin{cases} A_{k+1} = X_k + \dfrac{\tau_{k+1} - \tau_k}{\tau_{k+2} - \tau_k}(X_{k+2} - X_k) \\ L_k = \dfrac{X_k + A_k}{2},\ k = 1, 2, \ldots, M-2 \end{cases} \tag{12}$$

(3) A triple spline function was fitted to all $L_k(k = 1, 2, \ldots, M)$ to obtain the mean curve $\mathrm{m}_i(\mathrm{t})$, and it was separated from $\mathrm{r}_i(\mathrm{t})$

$$\mathrm{I_i(t)} = \mathrm{r_i(t)} - \mathrm{m_i(t)} \tag{13}$$

Compared with other adaptive time-frequency analysis methods such as empirical modal decomposition and local mean decomposition, LCD has superiority in terms of computation time, reduction of fitting error, and improvement of component accuracy, etc. Specific comparison results can be found in the literature [15].

4 Pilot Study

4.1 Test System and Conditions

When a hydraulic system operates, it generates various kinds of dynamic information. In order to study the relationship and characteristics of various types of dynamic information and to find a suitable condition monitoring method for hydraulic power systems, we designed a test system as shown in Figure 6 according to the common patterns and operating characteristics of hydraulic power systems in mechanical engineering.

In Figure 6, the motor 13 drives the gear pump 9 through the flexible coupling 11, and the outlet pressure of the oil pump is adjusted by the relief

Figure 6 Hydraulic system.

valve 4, relying on the adjustment of the working pressure of the relief valve to make the oil pump and the motor bear the shock load, and the load size is proportional to the working pressure of the relief valve. For the electro-mechanical information issued by the test device, eddy current and piezoelectric vibration sensors, oil pressure, temperature and flow sensors, sound level meters, current transformers, etc. were installed to obtain a total of eight types of electro-mechanical information sensors [21].

By setting the system operation status of the motor and oil pump and changing the installation position, the common system operation status of the hydraulic power system can be simulated on the test system so that the changes in the output signal characteristics of each sensor can be observed and analyzed.

4.2 Test Results

Figures 7, 8 and 9 show the results of four tests of the current power spectrum when the system occurs in the motor system operation state, the mechanical system operation state and the oil pump system operation state, respectively. Table 1 gives the 10 standard characteristic values (dB) of the current power spectrum in the four states.

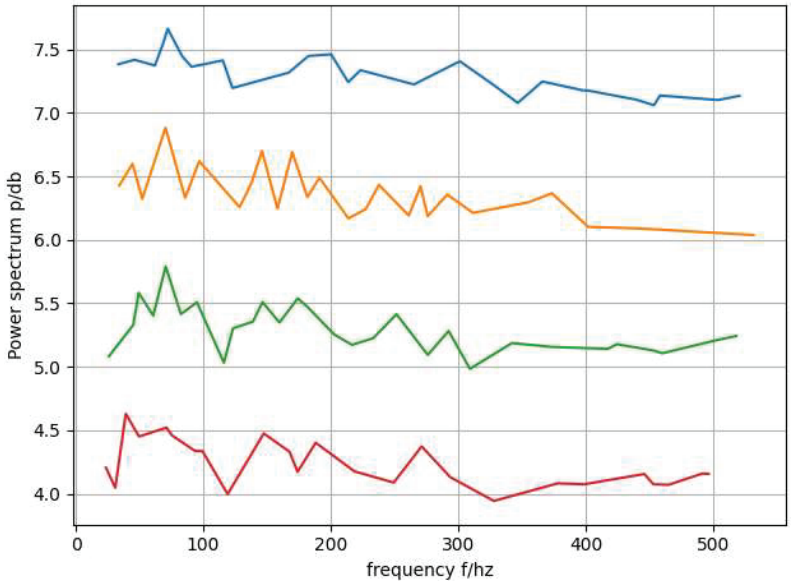

Figure 7 Current power spectrum during motor system operation.

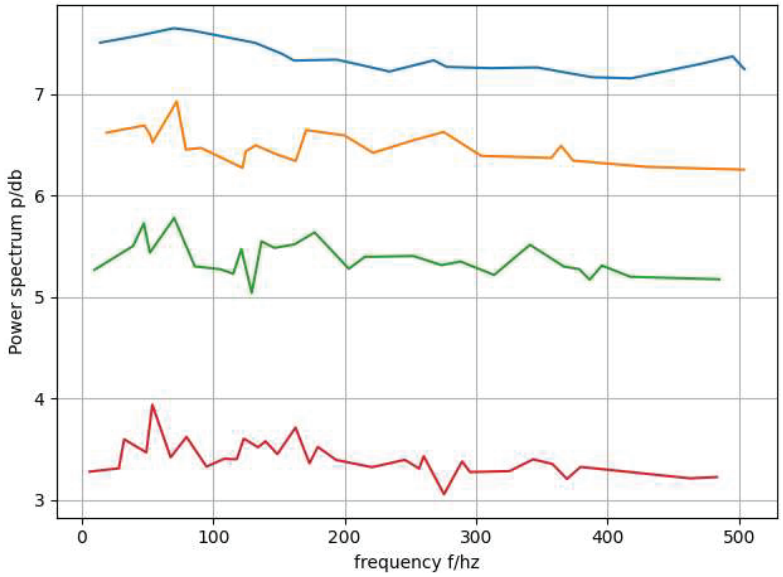

Figure 8 Current power spectrum during mechanical system operation.

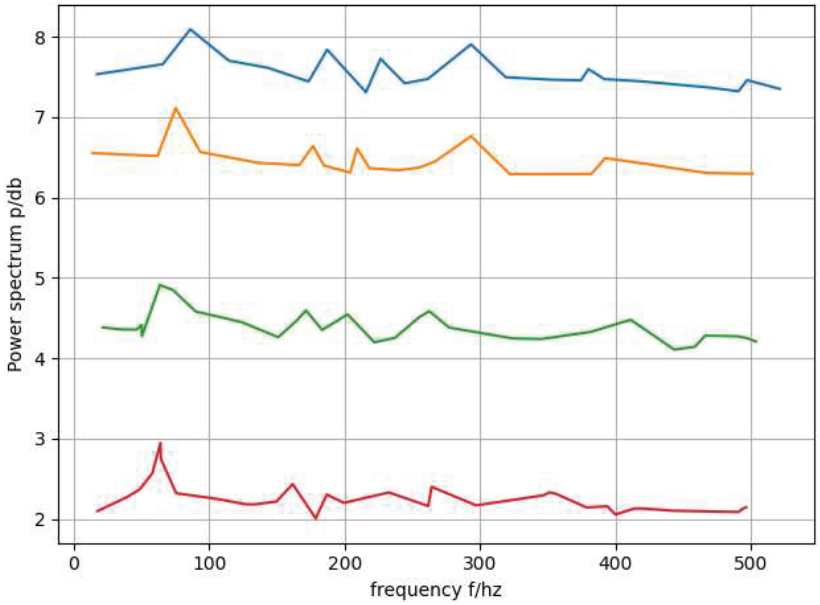

Figure 9 Current power spectrum of the oil pump system during operation.

Table 1 Eigenvalues of current signal power spectrum

Frequency f/Hz	26.6	50.0	73.4	100	126	150	174	200	250	350
Status 1	−26	7.7	−28	−32	−30	−17	−30	−34	−24	−31
Status 2	−14	11.1	−17	−26	−31	−61	−25	−28	−29	−28
Status 3	−24	8.5	−26	−17	−40	−20	−28	−41	−34	−24
Status 4	−29	7.5	−33	−34	−34	−34	−29	−32	−36	−32

As can be seen from Table 1: In the normal state, the current power spectrum has components at 50 Hz, 150 Hz and 250 Hz, which are the 1st, 3rd and 5th harmonic components of the current frequency (50 Hz), respectively. Comparing Figures 7 and 8, the most obvious difference between the mechanical system operation and the motor system operation is that the spectrum value on the right side is significantly larger than the spectrum value on the left side at the third harmonic (150 Hz). It can be seen from Figure 9: when the oil pump is operated in the internal drainage system, the side frequency components on both sides of the 1st and 3rd harmonics disappear. The above test results show that: different operating states correspond to different current power spectra, and the repeatability is very good under the same test conditions; therefore, the current spectrum can be used to identify the operating state of the hydraulic power system and lay the foundation for further research on the system operating state diagnosis method.

4.3 Application Examples

The HBT30 concrete pump produced by a factory had poor coaxiality after the main motor was connected to the rotating shaft of the triplex oil pump due to unqualified coupling processing, resulting in abnormal operating noise, vibration and no-load resistance of the hydraulic power system. Figure 10 shows the power spectrum of the A and B phases of the main motor of the concrete pump, with 500 lines per graph.

Let the vector array consisting of the standard mode eigenparameters of the current power spectrum of the hydraulic power system acquired in the test system be

$$x_{ri} = \begin{bmatrix} x_{r1} \\ x_{r2} \\ x_{r3} \\ x_{r4} \end{bmatrix} = \begin{bmatrix} x_{r1}(1), & x_{r1}(2) & \cdots & x_{r1}(500) \\ x_{r2}(1), & x_{r2}(2) & \cdots & x_{r2}(500) \\ x_{r3}(1), & x_{r3}(2) & \cdots & x_{r3}(500) \\ x_{r4}(1), & x_{r4}(2) & \cdots & x_{r4}(500) \end{bmatrix} \tag{14}$$

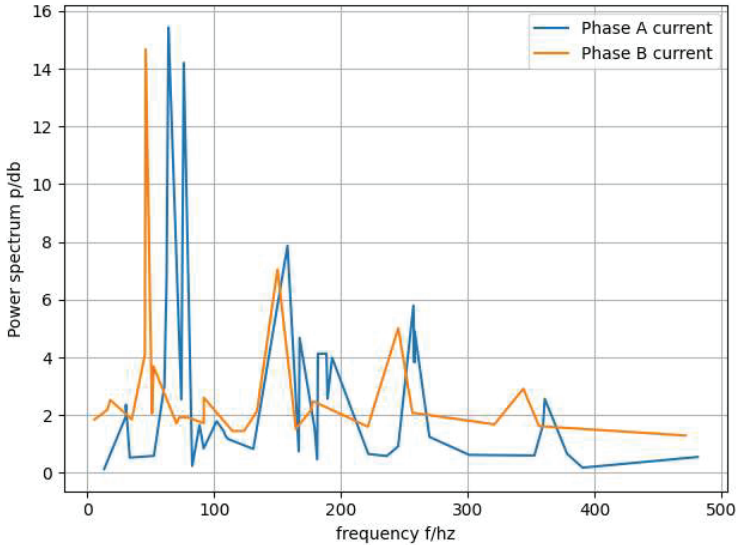

Figure 10 HBT30 concrete pump main motor current signal power spectrum.

The subscript $x_{r1}, x_{r2}, x_{r3}, x_{r4}$ indicates the standard mode of hydraulic power system in 4 states respectively, and 500 indicates the number of characteristic parameters of each standard mode.

5 Conclusions

The theoretical analysis and tests in this paper show that; due to the coupling of the rotor system, the mechanical, electrical and hydraulic signals of the hydraulic power system are correlated, and the degree of correlation is determined by the nature of the load; compared with the dynamic signals such as vibration and oil pressure, the current signal is the most sensitive to the operating state of the hydraulic power system, and has the advantages of smoothness, high signal-to-noise ratio and easy access. The greater the load of the hydraulic power system, the more obvious the operating state characteristics of the system in the current power spectrum. In the current power spectrum, the mechanism that the side frequency (side frequency bandwidth is equal to motor speed) components appearing on both sides of the 1st, 3rd and 5th harmonic components of current frequency (50 Hz) change with the motor load and the type of system operation state is not clear, and needs further study.

Acknowledgment

Scientific Research Fund of Hunan Provincial Education Department (No. 20B390).

References

[1] Coogan, C. G., and He, B. (2018). Brain-computer interface control in a virtual reality environment and applications for the internet of things. IEEE Access, 6, 10840–10849.

[2] Zubrycki, I., Kolesiński, M., and Granosik, G. (2017, June). Graphical programming interface for enabling non-technical professionals to program robots and internet-of-things devices. In International Work-Conference on Artificial Neural Networks (pp. 620–631). Springer, Cham.

[3] Ray, P. P. (2018). A survey on Internet of Things architectures. Journal of King Saud University-Computer and Information Sciences, 30(3), 291–319.

[4] Kougianos, E., Mohanty, S. P., Coelho, G., Albalawi, U., and Sundaravadivel, P. (2016). Design of a high-performance system for secure image communication in the internet of things. IEEE Access, 4, 1222–1242.

[5] Jo, D., and Kim, G. J. (2016). ARIoT: scalable augmented reality framework for interacting with Internet of Things appliances everywhere. IEEE Transactions on Consumer Electronics, 62(3), 334–340.

[6] García, C. G., Meana-Llorián, D., G-Bustelo, B. C. P., Lovelle, J. M. C., and Garcia-Fernandez, N. (2017). Midgar: Detection of people through computer vision in the Internet of Things scenarios to improve the security in Smart Cities, Smart Towns, and Smart Homes. Future Generation Computer Systems, 76, 301–313.

[7] Barricelli, B. R., and Valtolina, S. (2017). A visual language and interactive system for end-user development of internet of things ecosystems. Journal of Visual Languages & Computing, 40, 1–19.

[8] Pang, Z., Zheng, L., Tian, J., Kao-Walter, S., Dubrova, E., and Chen, Q. (2015). Design of a terminal solution for integration of in-home health care devices and services towards the Internet-of-Things. Enterprise Information Systems, 9(1), 86–116.

[9] Malik, P. K., Sharma, R., Singh, R., Gehlot, A., Satapathy, S. C., Alnumay, W. S.,... and Nayak, J. (2021). Industrial Internet of Things and its applications in industry 4.0: State of the art. Computer Communications, 166, 125–139.

[10] Yang, A., Zhang, C., Chen, Y., Zhuansun, Y., and Liu, H. (2019). Security and privacy of smart home systems based on the Internet of Things and stereo matching algorithms. IEEE Internet of Things Journal, 7(4), 2521–2530.

[11] Rubio-Drosdov, E., Díaz-Sánchez, D., Almenárez, F., Arias-Cabarcos, P., and Marín, A. (2017). Seamless human-device interaction in the internet of things. IEEE Transactions on Consumer Electronics, 63(4), 490–498.

[12] Premsankar, G., Di Francesco, M., and Taleb, T. (2018). Edge computing for the Internet of Things: A case study. IEEE Internet of Things Journal, 5(2), 1275–1284.

[13] Lindley, J., Coulton, P., and Cooper, R. (2017). Why the internet of things needs object orientated ontology. The Design Journal, 20(sup1), S2846–S2857.

[14] Castaño, F., Beruvides, G., Villalonga, A., and Haber, R. E. (2018). Self-tuning method for increased obstacle detection reliability based on internet of things LiDAR sensor models. Sensors, 18(5), 1508.

[15] Li, H., Ota, K., and Dong, M. (2018). Learning IoT in edge: Deep learning for the Internet of Things with edge computing. IEEE network, 32(1), 96–101.

[16] Rose, K., Eldridge, S., and Chapin, L. (2015). The internet of things: An overview. The internet society (ISOC), 80, 1–50.

[17] Lee, C. K., Lv, Y., Ng, K. K. H., Ho, W., and Choy, K. L. (2018). Design and application of Internet of things-based warehouse management system for smart logistics. International Journal of Production Research, 56(8), 2753–2768.

[18] An, P., Wang, Z., and Zhang, C. (2022). Ensemble unsupervised autoencoders and Gaussian mixture model for cyberattack detection. Information Processing & Management, 59(2), 102844.

[19] Silverio-Fernández, M., Renukappa, S., and Suresh, S. (2018). What is a smart device? – a conceptualisation within the paradigm of the internet of things. Visualization in Engineering, 6(1), 1–10.

[20] Savaglio, C., Ganzha, M., Paprzycki, M., Bădică, C., Ivanović, M., and Fortino, G. (2020). Agent-based Internet of Things: State-of-the-art and research challenges. Future Generation Computer Systems, 102, 1038–1053.

[21] Bai, T. D. P., and Rabara, S. A. (2015, August). Design and development of integrated, secured and intelligent architecture for internet of things and cloud computing. In 2015 3rd International Conference on Future Internet of Things and Cloud (pp. 817–822). IEEE.

Biographies

Rundong Shen received his B.Sc. degrees in Motor Vehicle Service Engineering from Changsha University of Science and Technology, China; M.Sc. degree in Transportation Engineering from Changsha University of Science and Technology, China; Now, Rundong Shen is a lecturer at Hunan Railway Professional Technical College, China; His research field of centers on machinery design and manufacture.

Kechang Zhang received his B.Sc. degrees in Mold design and manufacture from Xiangtan University, China; Now, Kechang Zhang is associate professor at Hunan Railway Professional Technical College, and he is a National technical experts, China; His research field of centers on machine design.

Jinyan Shi received her B.Sc. degrees in Machine Design and Automation from Lanzhou Jiaotong University, China; M.Sc. degree in Drive Technology and Intelligent System from Southwest Jiaotong University, China; Now, Jinyan Shi is an associate professor at Hunan Railway Professional Technical College, and she is a key young teacher in Hunan Province, China; Her research field of centers on CFD.